Hearing Research, 15 (1984) 187–195
Elsevier

HRR 00523

The central auditory pathway of the gerbil *Psammomys obesus*: A deoxyglucose study

Peter Melzer *

AK NRP, Zoologisches Institut der J.W. Goethe Universität, Siesmayerstr. 70, 6000 Frankfurt am Main, F.R.G., and Institute of Anatomy, University of Lausanne, Rue du Bugnon 9, 1011 Lausanne, Switzerland

(Received 25 January 1984; accepted 13 June 1984)

The tonotopic organization of the central auditory pathway of the gerbil *Psammomys obesus* was mapped with deoxyglucose autoradiography under anesthesia. Animals, injected with tritiated deoxyglucose, were stimulated with 0.8, 2.5 and 17.0 kHz tone bursts monaurally in the free field and compared with non-stimulated controls. Apart from the medial geniculate body, all auditory structures showed sound-specific uptake of tracer. Frequency selective tracer accumulation could not be discriminated in the auditory cortex, the nuclei of the lateral lemniscus or the superior olivary complex. Isofrequency laminae could be determined most precisely in the dorsal cochlear nucleus and the central nucleus of the inferior colliculus. About half the mass of each of these nuclei is devoted to the processing of sound below 2.5 kHz. This disproportionately large representation of low frequencies matches the very high sensitivity of the peripheral auditory system in that range.

central auditory pathway, *Psammomys obesus*, tonotopy, deoxyglucose autoradiography

Introduction

The deoxyglucose (DG) autoradiographic method was developed to measure the local metabolism rate of glucose in brain structures [9]. Since neuronal energy consumption seems to be mainly associated with sodium pump activity [12], the method can be used for studying stimulus-evoked neuronal activity, and, in particular, sensory responses. In the auditory system of rodents, gross elevated metabolism was shown in the IC of conscious rats exposed either uni- or bilaterally to ambient laboratory noise [27]. Frequency-selective DG uptake corresponding to the tonotopic organization of mammals could be demonstrated in the central auditory pathway of the conscious mongolian gerbil; as a peculiarity, alternating laminae of high and low activation underlie tonotopic responses in the ICC [24]. No findings, which correspond to this observation, are available from electrophysiological studies. The phenomenon was not observed in anesthetized cats; in their ICC, only a single layer of increased DG uptake was obtained for a distinct tone frequency. The layer's location was in agreement with best frequency recordings [26]. In our laboratory, previous DG studies with conscious, restrained gerbils showed that stimulus-evoked responses were indiscernible from spontaneous activation levels [13]. Therefore, animals under anesthesia were used for this study. It was carried out to reveal the distribution of frequency-specific responses in the central auditory pathway of the sand rat (*Psammomys obesus*) with DG autoradiography. The sand rat, a gerbilline species, lives in semi-arid deserts of Northern Africa. It is considered to be a member of the *Meriones* group [11].

Materials and Methods

For each stimulus frequency, three adult male sand rats, 8–24 weeks old, 127–180 g body weight, deprived of food for 24 h, were used. In addition, two unstimulated animals served as controls. In a sound-attenuated chamber, sound was applied to

* *Present address*: Institute of Anatomy, University of Lausanne, Rue du Bugnon 9, CH-1011 Lausanne, Switzerland.

the left ear; the right ear canal was occluded with a histoacrylate plug. Dynamic loudspeakers were used for the two lower frequencies and an electrostatic loudspeaker for 17.0 kHz stimulation; tone burst stimuli (repetition rate 5/s, burst duration 50 ms, rise and fall time 5 ms) were generated with a wave generator, driven by a pulse generator. Intensity was set with a decade attenuator. In the 0.8 kHz experiments, two sand rats were stimulated with 80 dB SPL; at this intensity there was a 2.4 kHz harmonic, attenuated by at least 60 dB. One animal received sound at 60 dB SPL. In the 2.5 kHz experiments, all animals were stimulated with 60 dB SPL; in the 17.0 kHz experiments, 80 dB SPL were used exclusively. The stimulus was monitored with a spectrum analyzer (Ubiquitous UA-500A, Federal Scientific) and a measuring amplifier (Brüel and Kjaer, model 2610). Body temperature was maintained with an electric heating pad. All animals were anesthetized with enflurane (Ethrane, Ohio Medical Prod.), which was maintained at 3.0% during stimulation. At that concentration, no epileptogenic convulsions were observed. Tone bursts were started simultaneously with tracer application. 2-[1,2-^{3}H]Deoxy-D-glucose, specific activity ca. 40 Ci/mmol (New England Nuclear), in saline was injected i.v. (400 μCi/100 g body weight). In one experimental set, a 2.5 kHz stimulated animal and a control were injected i.v. with 3-ortho-[^{3}H]methyl-D-glucose, specific activity 80 Ci/mmol (New England Nuclear), at equal dose and concentration. This compound is taken up by neurons and glia, but is not a substrate for hexokinase. Thus, differential accumulation of DG and orthomethylglucose (MG) is an indicator of glucose transport and metabolism. The animals were decapitated 45 min after injection. Their heads were embedded in semi-liquid carboxymethylcellulose and immediately deep-frozen onto cryostat object holders in liquid nitrogen. The orientation of their rostrocaudal axes was approximately perpendicular to the holder plane, their noses pointing up. Coronal sections, 20 μm thick, were cut on a model 450 MP cryo-microtome (PMV) at $-25\,^{\circ}$C, using Ullberg's technique [28]. Sections were gently freeze-dried by storing in the cryostat cabinet for three days. They were then exposed to LKB Ultrofilm ^{3}H for 4 weeks. The sections were kept in close contact with the film in sealed, evacuated, light-proof plastic bags (method adopted from [10]). The spatial resolution power of this approach and further technical details have been reported elsewhere [14]. After adjustment to room temperature and film development, autoradiograms of corresponding regions were evaluated with bright-field microscopy. Since counterstaining of the tape-based sections could not be achieved with sufficient quality, auditory structures were specified by comparison with separate series of Nissl- or Klüver/Barrera-stained paraffin sections, which were available in all three anatomical planes. Optical density levels were measured with a microdensitometer (Zeiss) based on a Polyvar microscope (Reichert and Jung). It was set at 50×150 μm diaphragm aperture and zeroed to autoradiogram background. Magnification was three-fold. For each region of interest, at least six independent readings/autoradiogram were taken. Optical density means from autoradiograms (three per animal) were compared with those of adjacent and homotopic contralateral regions using Student's t-tests. Regions with significantly increased DG accumulations ($P = 0.01$) were considered as activated. Ratios of activated versus non-activated tissue were calculated for inter-animal comparison.

Whole head sectioning permitted freezing of the brains with a negligible lag of postmortem time. Furthermore, the technique provides the possibility of cutting sections of the brain as it is oriented within the skull. There was no brain deformation and negligible shrinkage. Oblique lateral deviations from the coronal plane could be minimized by adjusting the cryotome stage so that the cutting plane paralleled the caudal ends of the eye balls and lenses. Determined from the caudal ends of the cortex and the IC, left end-versus-right end shifts were smaller than 100 μm. The dorso-ventral deviation from the coronal plane about the latero-lateral axis could not be compensated. Yet, a reproducible cutting plane could be established. Thus, the three-dimensional reconstruction of regions of interest was feasible. We attempted that by manual drawing (Fig. 3), which is a rather crude approach. However, done more accurately with computer aid, the reconstructions can serve as stereotaxic guidance for electrophysiological studies.

Results

None of the effects described below could be observed in the two experiments with MG as tracer. There was only a distinct difference of tracer accumulation between gray and white matter. The optical density level of gray matter structures was uniform (Fig. 2E).

Stimulus-evoked responses could be revealed in all auditory structures apart from the medial geniculate body. No frequency-specific responses were found in the superior olivary complex, lateral lemniscus, and auditory cortex. Therefore, only results concerning the CN and the IC are presented.

The cochlear nucleus

The CN of *Psammomys obesus* was parcellated into its subnuclei using cytoarchitectonic criteria defined in cats [19] and mice [30]. For comparison with other terminologies, the reader may refer to Brawer et al. [1]. Nuclear volumes were estimated as follows. The areas of photographic enlargements of autoradiograms were measured with the aid of a graphics tablet (Morphomat 10, Zeiss). The volumes to be determined were split into several subvolumes between the measured areas, each subvolume being equal to the mean of the areas of its two end-planes multiplied by the distance between them. The sum of all subvolumes gave the estimated nuclear volume. The volume of the DCN was 0.22 mm^3 ($n = 6$), and that of the total CN 1.17 mm^3 ($n = 6$). Hence, the DCN was 3.78-fold larger than the ventral cochlear nuclei.

In all animals, there were high levels of DG accumulation in both CN, but stimulus-specific optical density increases were observed only in the CN ipsilateral to the stimulated ear. Regions of activated neurons could be resolved over all layers of the DCN, but were most pronounced over its granular layer (Fig. 1A). Neurons activated by the

Fig. 1. Activation patterns of the DCN ipsilateral to sound source. Photomicrograph of a frontal Nissl-stained paraffin section (A); typical autoradiograms of a 17.0 kHz stimulated (B), a 2.5 kHz stimulated (C), and a control animal (D). Bar in A indicates 500 μm. Dorsal is up, lateral is right. Note elevated DG uptake elicited dorsally with 17.0 kHz and further ventrally with 2.5 kHz stimulation (arrows). Sg accumulated more DG than Sm or Sc.

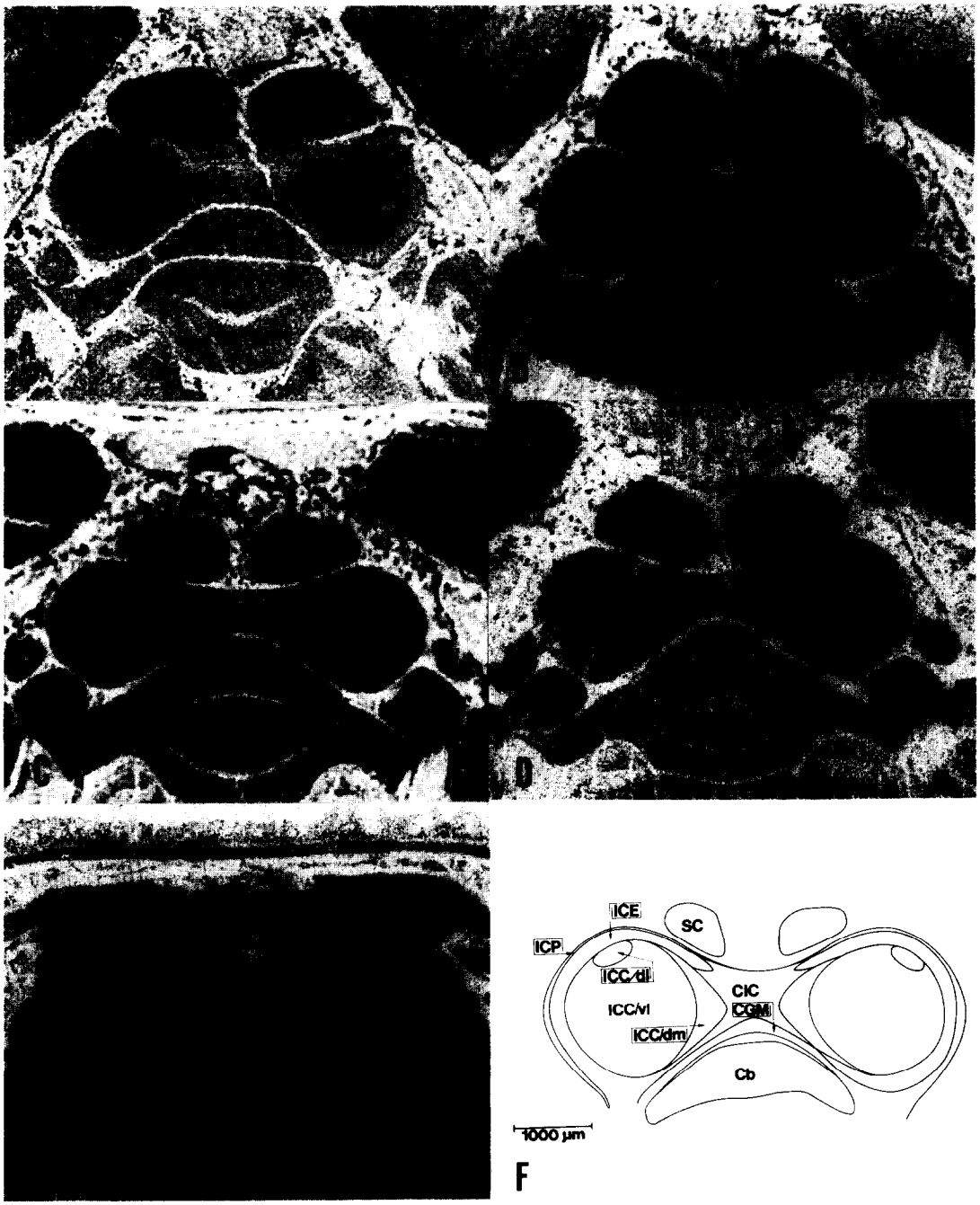

Fig. 2. Activation patterns within the IC: Partial photographic enlargements of autoradiograms of corresponding whole head sections showing 17.0 kHz (A), 2.5 kHz (B), 0.8 kHz stimulus responses (C), a non-stimulated control (D), and an animal, injected with MG instead of DG and receiving 2.5 kHz sound (E). The line drawing (F) specifies morphology derived from Nissl-stained sections and autoradiographic images. The cutting plane is coronal under the limitations stated in Materials and Methods. The dorsal–ventral axis of the sections runs from top to bottom; the caudal–rostral axis runs towards the viewer, left is right (CIC, commissure of the IC; CGM, central gray matter; Cb, cerebellum; SC, superior colliculus). Note the ventromedial-to-dorsolateral frequency-specific layer shift in the ICC. Slight activation in the dorsal IC, visible in A and D, is due to background low frequency noise. In contrast to D, the dorsolateral activation in C forms a distinct band. The almost uniform optical density pattern in E raises evidence that high gray levels in A to D express increased neuronal/glial metabolism.

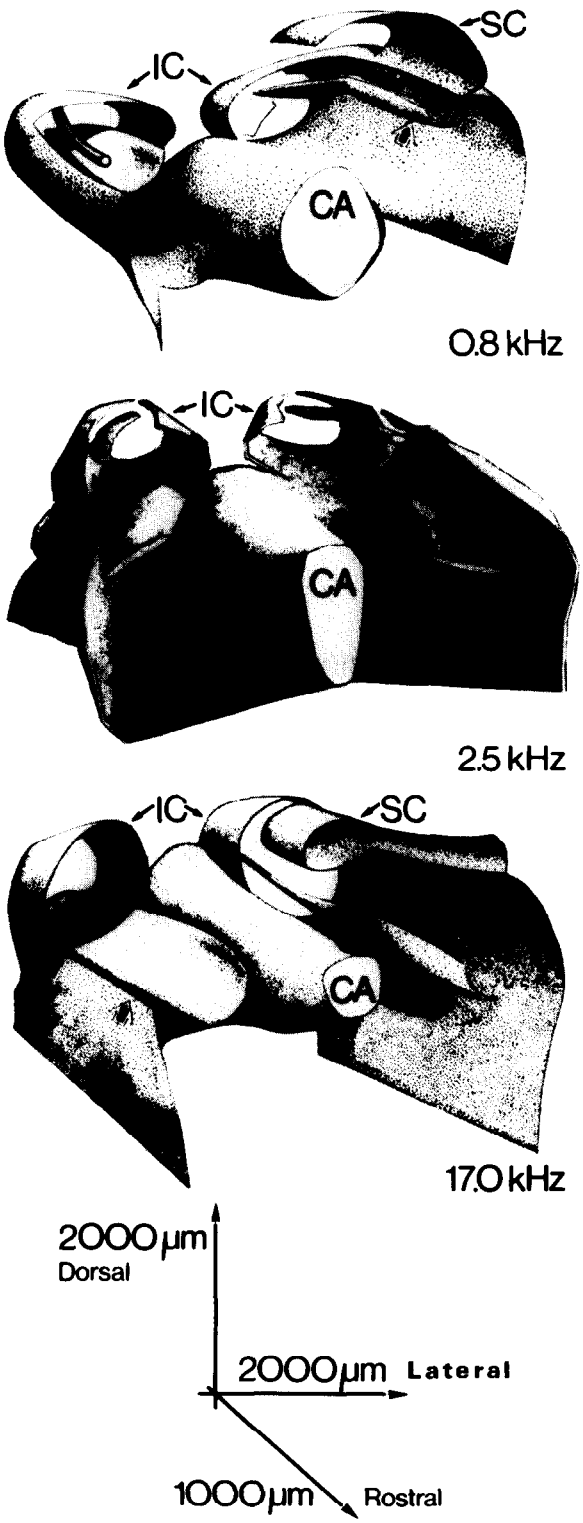

17.0 kHz stimulus were situated in the far dorsomedial edge of the nucleus (Fig. 1B), whereas 2.5 kHz responding neurons were located near its center (Fig. 1C). Each region covered a large part of the DCN (up to 20%). All spanned the nucleus' rostrocaudal extent entirely (ca. 600 µm). 0.8 kHz activation could not be detected with certainty. In the control, DG uptake was elevated in the granular layer, but it was uniform (Fig. 1D). In the ventral cochlear nuclei, 0.8 and 2.5 kHz induced DG uptake was very weak. A tonotopic pattern of response could not be identified properly.

The inferior colliculus

From Nissl- and Klüver/Barrera-stained section series, the IC was segregated into its nuclei and divisions closely following the cytoarchitectonic definitions applied to cats by Rockel and Jones [21,22]. The brachium and the commissure of the IC could be discerned. The ICC was clearly distinguishable including its divisions, i.e. the ICC/dm, the ICC/vl, and even a dorsolateral region of higher cell density, the ICC/dl. However, difficulties arose when boundaries of the adjacent ICE and ICP had to be defined. I confined the ICP to the most peripheral cellular layers of the IC, forming a narrow sheath (150 µm) of small round cells. Inside these, there are layers of closely packed larger cells (> 20 µm), which become more widely spaced further interiorly at the line of transition into the ICC. We interpreted the region of packed large cells to be the ICE. It comprises the interior part of the lateral zone as well as the parabrachial region defined by van

Fig. 3. Three-dimensional reconstruction of zones of frequency-induced high DG uptake within the ICC (large arrows) and the ICE (small arrows), drawn from autoradiograms of a series of whole head sections (one image/100 µm). The rostral-caudal dimension is expanded twofold. In the ICC, stimulus-evoked activations form distinct laminae, which are layered on top of each other, the 17.0 kHz lamina being most ventromedially and the 0.8 kHz lamina most dorsolaterally. In the medial–lateral direction, the 17.0 kHz lamina is aligned with the curvature of the nucleus' boundary. In contrast, both low frequency laminae are straight. In the caudal–rostral direction, all three laminae undergo a rostral, ventral and medial tilt. Only the two lower frequencies evoked activity in a tubular region of the dorsolateral ICE. A tonotopy could not be determined there (CA, central aqueduct; SC, superior colliculus).

Noort [29] in cats. Its boundaries with the ICC and ICP could be determined best on DG autoradiograms.

The peripheral ICP was visible as a zone of uniform stimulus-independent DG accumulation. A thin rim of elevated optical density surrounded the ICC laterally, dorsally, and ventrally. Bands of high DG uptake evoked by stimulation did not spread over that line. In the 0.8 and 2.5 kHz stimulated animals, there were significantly activated regions, ca. 100 μm in diameter, in the dorsolateralmost IC on both sides (Fig. 2B and C). The optical density increase on autoradiograms was 1.9-fold. I assigned this activation to the ICE, since it was clearly outside the uniform tracer level of the ICP, and outside of the ICC. These 'hot spots' of activation could not be found in high frequency-stimulated and control animals (Fig. 2A and D). Hence, based on differential DG accumulation, I was able to draw functional borders between the nuclei of the IC. Frequency-specific bands of high DG accumulation were revealed in the ICC/vl and ICC/dl ipsi- and contralateral to the stimulated ear (Fig. 2). Viewed transversely, they appeared to be confined to laminae similar to the pattern outlined in the study of Rockel and Jones [21]. This was particularly true for the layer elicited by 17.0 kHz. The laminae did not cover the total spans of the hypothetical concentric 'onion shells' [21], but merely their ventral portions. From these bands, three-dimensional layers could be reconstructed (Fig. 3). Their widths ranged from 550 to 1100 μm, and their thicknesses varied from ca. 110 μm (0.8 and 17.0 kHz) up to 150 μm (2.5 kHz). Optical densities were not homogeneously distributed across the layers' thicknesses. In each layer, the activation was greatest at its midline, decreasing towards each side. On average, their rostrocaudal extents were 1300 μm. With increasing frequency, the layers shifted from dorsolateral to ventromedial. Their rostral and caudal ends were not strictly aligned above each other. Low frequency layers began more caudally. The interlayer shift was ca. 200 μm. Reciprocally, the 0.8 kHz stimulus layer vanished ca. 300 μm posterior of the termination of the 2.5 kHz stimulus layer, which was in turn situated 300 μm posterior of the rostral boundary of the 17.0 kHz stimulus layer. All three layers underwent a steep deflection ventromedially. The animals receiving 80 dB SPL sound at 0.8 kHz exhibited a second activated lamina ventral to the 0.8 kHz layer and located in the region of the 2.5 kHz responses. The second activation was only very faint in the ICC of the animal stimulated with 60 dB (SPL) sound (Fig. 2C). The ratio of contralateral versus ipsilateral activation was about 1.3 at 2.5 kHz, 60 dB SPL, whereas its activity increase was 2.7-fold, if compared with non-activated regions within the ICC. The ICC/dm was moderately activated in all stimulated animals. Brachium and commissure of the IC exhibited significantly lower DG uptake. In the control animals, weak but widespread elevated DG accumulation occurred in the dorsal IC. Apart from that, no increase of optical densities was indicated in any of the other IC regions.

Discussion

The cochlear nucleus

Apparently, the stimuli activated both ears and both CN. The most prominent osseous structures in the gerbilline skull are the tremendously enlarged bullae [4], which almost touch each other in the center of the skull. The bilateral activation observed in all structures of the central auditory pathway may be due to crosstalk between the bullae.

Sound spectrum monitoring revealed that the experimental chamber did not entirely suppress low frequency noise. The residual intensity levels were sufficient to stimulate low frequency neurons, which may account for the faint, but apparently increased activity in the CN and the IC in control as well as high frequency-stimulated animals.

Volumes and dorsal/ventral nucleus volume ratios, calculated for the entire CN and its divisions, closely parallel the values reported for the mongolian gerbil [6]. Therefore, the morphometric technique, which was equally applied for tonotopy measurements, is sufficiently accurate.

The inferior colliculus

In the ICE and ICP, there was no indication of a precise tonotopic organization, although a part of the dorsolateral ICE preferred low frequency stimulation. In the squirrel monkey, virtually all

the auditory neurons in these nuclei are broadly tuned, preferring low frequencies (< 4 kHz [5]). This contrasts with a tentative report of tonotopy in the ICE of the cat [23]. A parcellation of the region of the ICE and ICP as defined by Morest and Oliver [16] could not be confirmed.

The absence of tonotopic response within the ICC/dm is consistent with findings in anesthetized cats [15]. My results do not indicate any functional differences between ICC/dl and ICC/vl. They obviously form a tonotopical unit. An even further distinction of the ICC into more subdivisions with multiple tonotopic maps [18] is not supported. The ICC of the cat exhibits a laminated organization [9]. These laminae are composed of afferent fibers and the dendritic fields of disc-shaped cells [18]. It is not clear whether the frequency-specific layers reconstructed in this study represent pre- or postsynaptic activation or both. However, they strongly support a laminar organization of the ICC of the sandrat as described by Rockel and Jones in the cat [21]. In contrast to the observation of Oliver and Morest in the cat [18] that the laminae maintain their relative positions with respect to the longitudinal meridians of the subdivisions of the ICC, the activity layers undergo a steep ventral tilt rostrally (Fig. 3). Their general shape matches reconstructions drawn from multi-unit recordings in the squirrel monkey to a surprisingly detailed extent [5]. Layer thicknesses determined from autoradiograms closely approach the height of dendritic fields of the bitufted principal cells of Rockel and Jones [21] and of the disc-shaped cells of Oliver and Morest [18] in the cat ICC. The contra-to-ipsilateral activation ratio resembles that found with measurements of local metabolic rate of glucose in conscious rats [8]; the activated-to-non-activated tissue ratio was even 25% higher. The laminae were symmetric and exhibited only slight uni- or bilateral discontinuities. Their unequal activation levels may reflect that ca. 75% of ascending IC inputs arise from contralateral brain stem nuclei in the gerbil [17].

I have attempted to calculate how the amount of ICC tissue and the corresponding length of basilar membrane vary with frequency for different species in comparison with the sand rat. In Fig. 4, the depth beneath the dorsal surface of the

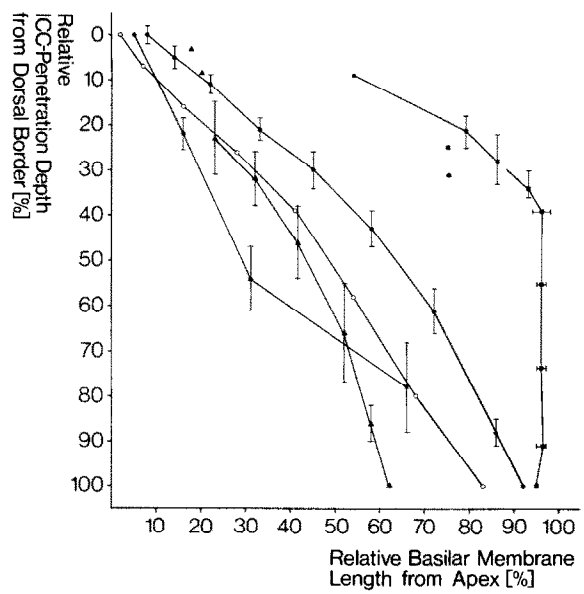

Fig. 4. Plot of relative depth in ICC (as percentage of the total depth within which acoustic neurons were recorded) as a function of relative distance along the basilar membrane from apex corresponding to the same frequency (as percentage of total length along basilar membrane). Functions are plotted for the albino rat (▲), the cat (●), the squirrel monkey (○), the greater horseshoe bat (■), and the sand rat (*). Apart from the sand rat, values for penetration depths and corresponding best frequencies were obtained from electrophysiological data on the rat [2], the cat [15], the squirrel monkey [5] and the echolocating bat [20]. Relative depths in the plot for the sand rat were derived from averaged ICC area measurements on autoradiograms, except for the lowest frequency (ca. 0.2 kHz), whose value was determined from multi-unit recordings (unpub. obser.). In the plots for the cat and bat, bars indicate extremes, whereas in the plots for the rat and sand rat, they express standard deviation. Data for the relative basilar membrane length corresponding to a certain frequency were calculated from a conversion function developed by Greenwood [7].

ICC at which a given frequency was represented is plotted against that frequency's position on the basilar membrane. Using data from various electrophysiological studies (see legend), relative penetration depths have been plotted as a function of frequency. Frequency has been related to its approximate locus of representation on the basilar membrane (in per cent of its total length) with a function developed by Greenwood [7]. None of the resulting curves is completely straight, but the slopes change only little for the rat, cat, and squirrel monkey. The curve for the echolocating

bat changes drastically at 70 kHz and seems to be composed of two linear components. Apparently, this is the result of an extraordinarily increased volume of ICC devoted to the processing of a comparably narrow frequency band [20].

In this study, areas dorsal and ventral to frequency-specific layers were used as parameter of relative amount of ICC devoted to the processing of a distinct frequency range (ICC/dm excluded). Morphometric assessment indicated that, on the average, 20% of the available collicular space processes frequencies up to 0.8 kHz ($n = 24$), 54% frequencies up to 2.5 kHz ($n = 28$), and, finally, 78% frequencies up to 17.0 kHz ($n = 26$). Measurements obtained from the animal stimulated with harmonics demonstrated that ca. 35% of the ICC volume covered the space between 0.8 and 2.4 kHz isofrequency laminae ($n = 10$). Therefore, three-quarters of the tissue processing frequencies lower than 2.5 kHz process tones within these 1.5 octaves exclusively. The plot of these values versus their according relative basilar membrane lengths features a steep slope up to 2.5 kHz, which turns into a more moderate increase between 2.5 kHz and 17.0 kHz. The change of slope is opposite to that of the slopes of all other curves displayed in Fig. 4. This result indicates a *disproportionately* large devotion of ICC volume to the processing of sound below 2.5 kHz in comparison with the other species.

The most prominent sensitivity maximum in the peripheral auditory system of the sand rat stretches from 0.5–4 kHz [11,25]. Sounds within this frequency range may be generated by the wing beat of attacking birds of prey [11] and infraspecific alert signals produced by hindleg drumming [3]. They may be important for preserving the species.

Morphometric measurements in the DCN showed that 52% of the tissue ventral to the 2.5 kHz activation must be devoted to processing of frequencies below 2.5 kHz. Obviously, a disproportionate distribution of frequency-selective neurons is already present at this level of the ascending pathway.

In summary, DG autoradiography of the central auditory pathway of sand rats under anesthesia has revealed frequency-specific laminae within the ICC and the CN. Morphometry indicates that a disproportionately large amount of ICC and DCN tissue processes frequencies in the range of this species' most significant auditory sensitivity maximum.

Abbreviations

CN	cochlear nucleus
DCN	dorsal cochlear nucleus
DG	2-deoxy-D-glucose
IC	inferior colliculus
ICC	central nucleus of the inferior colliculus
ICC/dl	dorsolateral division of the central nucleus of the inferior colliculus
ICC/dm	dorsomedial division of the central nucleus of the inferior colliculus
ICC/vl	ventrolateral division of the central nucleus of the inferior colliculus
ICE	external nucleus of the inferior colliculus
ICP	pericentral nucleus of the inferior colliculus
MG	3-ortho-methyl-D-glucose
Sc	stratum centrale
Sg	stratum granulosum
Sm	stratum moleculare

Acknowledgements

This project was funded by the 'Deutsche Forschungsgemeinschaft' (SFB 45, B 41). I am indebted to the assistance, helpful comments and strong support of Dr. H.-M. Kellner, Dr. G. Kloss and Chr. Kötter of the Hoechst AG, Prof. Chr. Winter, Dr. W. Plassmann, A. Heidt, M. Kreuder, K. Grommet, M. Müller, and J. Schloos of the J.W. Goethe University. I thank Dr. P.G.H. Clarke, University of Lausanne, for his help in preparing the manuscript.

References

1 Brawer, J.R., Morest, D.K. and Cohen Kane, E. (1974): The neuronal architecture of the cochlear nucleus of the cat. J. Comp. Neurol. 155, 251–300.

2 Clopton, B.M. and Winfield, J.A. (1973): Tonotopic organization in the inferior colliculus of the rat. Brain Res. 56, 355–358.

3 Daly, M. and Daly, S. (1975): Behavior of *Psammomys obesus* (rodentia, gerbillinae) in the Algerian Sahara. Z. Tierpsychol. 37, 298–321.

4 Daniel, H.J., Fulghum, R.S., Brinn, J.E. and Barrett, K.A. (1982): Comparative anatomy of the eustachian tube and middle ear cavity in animal models for otitis media. Ann. Otol. Rhinol. Laryngol. 91, 82–89.

5 FitzPatrick, K.A. (1975): Cellular architecture and topographic organization of the inferior colliculus of the squirrel monkey. J. Comp. Neurol. 164, 185–208.

6 Frisina, R.D., Chamberlain, S.C., Brachman, M.L. and Smith, R.L. (1982): Anatomy and physiology of the gerbil cochlear nucleus: An improved surgical approach for microelectrode studies. Hearing Res. 6, 259–275.
7 Greenwood, D.D. (1961): Critical bandwidth and the frequency coordinates of the basilar membrane. J. Acoust. Soc. Am. 33, 1344–1356.
8 Huang, C., Dickson, J.W., Fex, J. and Sokoloff, L. (1981): Patterns of local cerebral glucose utilization in the inferior colliculus of the rat. Proc. Soc. Neurosci. 11, 57 (Abstract).
9 Kennedy, C., DesRosiers, M.H., Jehle, J.W., Reivich, M., Sharpe, F. and Sokoloff, L. (1975): Mapping of functional neural pathways by autoradiographic survey of local metabolic rate with [^{14}C]deoxyglucose. Science 187, 850–853.
10 Kloss, G., Kellner, H.M. and Kötter, Chr. (1973): Vakuum-Kontakt-Methode in der Makroautoradiographie. Z. Naturforsch. 28c, 468.
11 Lay, D.M. (1972): The anatomy, physiology, functional significance and evolution of specialized hearing organs of gerbilline rodents. J. Morphol. 138, 41–120.
12 Mata, M., Fink, D.J., Gainer, H., Smith, J.B., Davidson, L., Savaki, H., Schwartz, W.J. and Sokoloff, L. (1980): Activity-dependent energy metabolism in the rat posterior pituitary primarily reflects sodium pump activity. J. Neurochem. 34, 213–215.
13 Melzer, P. and Schloos, J. (in press): (H-3)-Deoxyglucose autoradiography on stimulus-specific response in the gerbilline auditory system in consciousness and under anesthesia.
14 Melzer, P. (1984): Whole head sectioning in [^{3}H]deoxyglucose mapping of auditory responses in gerbils. Brain Res. Bull. 12, 331–334.
15 Merzenich, M.M. and Reid, M.D. (1974): Representation of the cochlea within the inferior colliculus of the cat. Brain Res. 77, 397–415.
16 Morest, D.K. and Oliver, D.L. (1984): The neuronal architecture of the inferior colliculus in the cat: defining the functional anatomy of the auditory midbrain. J. Comp. Neurol. 222, 209–236.
17 Nordeen, K.W., Killackey, H.P. and Kitzes, L.M. (1983): Ascending auditory projections to the inferior colliculus in the adult gerbil, *Meriones unguiculatus*. J. Comp. Neurol. 214, 131–143.
18 Oliver, D.L. and Morest, D.K. (1984): The central nucleus of the inferior colliculus in the cat. J. Comp. Neurol. 222, 237–264.
19 Osen, K.K. (1969): Cytoarchitecture of the cochlear nuclei in cat. J. Comp. Neurol. 136, 453–484.
20 Pollak, G.D. and Schuller, G. (1981): Tonotopic organization and encoding features of single units in inferior colliculus of horseshoe bats: Functional implications for prey identification. J. Neurophysiol. 45, 208–226.
21 Rockel, A.J. and Jones, E.G. (1973): The neuronal organization of the inferior colliculus of the adult cat. I. The central nucleus. J. Comp. Neurol. 147, 11–60.
22 Rockel, A.J. and Jones, E.G. (1973): The neuronal organization of the inferior colliculus of the adult cat. II. The pericentral nucleus. J. Comp. Neurol. 149, 301–334.
23 Rose, J.E., Greenwood, D.D., Goldberg, J.M. and Hind, J.E. (1963): Some discharge characteristics of single neurons in the inferior colliculus of the cat. I. Tonotopical organization, relation of spike-counts to tone intensity, and firing patterns of single elements. J. Neurophysiol. 26, 294–320.
24 Ryan, A.F., Woolf, N.K. and Sharp, F.R. (1982): Tonotopic organization in the central auditory pathway of the mongolian gerbil: A 2-deoxyglucose study. J. Comp. Neurol. 207, 369–380.
25 Schmidt, R.A. and Zwislocki, J.J. (1977): Comparison of sound-transmission and cochlear-microphonic characteristics in mongolian gerbil and guinea pig. J. Acoust. Soc. Am. 61, 133–149.
26 Servière, J. and Webster, W.R. (1982): A combined electrophysiological and [^{14}C]2-deoxyglucose study of the frequency organization of the inferior colliculus of the cat. Neurosci. Lett. 27, 113–118.
27 Sokoloff, L. (1981): Localization of functional activity in the central nervous system by measurement of glucose utilization with radioactive deoxyglucose. J. Cereb. Blood Flow Metabol. 1, 7–36.
28 Ullberg, S. (1954): Studies on the distribution and fate of [S^{35}]-labelled benzylpenicillin in the body. Acta Radiol. Suppl. 118, 1–110.
29 Van Noort, J. (1969): The structure and connections of the inferior colliculus. An investigation of the lower auditory system. Van Gorcum and Co., Assen, The Netherlands.
30 Webster, D.B. and Trune, D.R. (1982): Cochlear nuclear complex of mice. Am. J. Anat. 163, 103–130.